

## Quantitative investigation of a terahertz artificial magnetic resonance using oblique angle spectroscopy

T. Driscoll,<sup>a)</sup> G. O. Andreev, and D. N. Basov

*Department of Physics, University of California, San Diego, La Jolla, California 92093*

S. Palit, Tong Ren, Jack Mock, Sang-Yeon Cho, Nan Marie Jokerst, and D. R. Smith

*Department of Electrical and Computer Engineering, Duke University, Durham, North Carolina 27708*

(Received 13 December 2006; accepted 17 January 2007; published online 2 March 2007)

The authors present a spectroscopic analysis of a planar split-ring-resonator (SRR) medium at terahertz frequencies, quantitatively characterizing the associated magnetic resonance. Experimental quantification at terahertz and infrared frequencies of metamaterial optical constants has been primarily absent, largely due to the difficulty of collecting phase information at these frequencies. In this letter, the authors circumvent the need for phase information in the characterization by acquiring the power transmitted through the metamaterial at a series of oblique angles, and relating the multiangle data set to the effective permittivity and permeability through the Fresnel expressions. The resulting measurements reveal the expected resonant permeability of the SRR which exhibits a range of negative values, the minimum value being  $\mu = -0.8$  at 1.1 THz. © 2007 American Institute of Physics. [DOI: 10.1063/1.2679766]

The rapidly growing field of metamaterials is based around the ability to create tailored electric and magnetic responses in a host material by the inclusion of designed geometric, usually conducting elements. If these elements are positioned with a periodicity  $P$ , sufficiently smaller than the wavelength of applied light  $\lambda$  ( $P < \lambda/5$ ), they can form an effective medium electromagnetically indistinguishable from a continuous material.<sup>1</sup> Artificial materials have generated particular interest for their ability to exhibit magnetic response at frequency ranges where magnetic response is usually absent. Magnetism in natural materials is a quantum mechanical phenomenon, occurring whenever a net electron spin imbalance or an orbital spin imbalance creates a magnetic moment. In contrast, metamaterial tailored in magnetism is quite different, resulting from a time-varying magnetic flux inducing resonant oscillatory electric currents along structured mesoscopic metallic inclusions.

Artificial magnetism has been well explored at microwave frequencies,<sup>2-4</sup> but a rigorous quantitative retrieval of the full optical constants has not yet been done at terahertz and infrared frequencies. This is due, in part, to the difficulty in fabricating three-dimensional bulk metamaterial structures, as well as difficulty in obtaining the complete phase information needed to retrieve the complex permittivity  $\epsilon$  and permeability  $\mu$  by way of direct inversion (known as the  $s$ -parameters method). At microwave frequencies, network analyzers are capable of obtaining the phases of both transmitted as well as reflected waves, enabling a retrieval procedure in which  $\epsilon$  and  $\mu$  can be determined. At optical frequencies, phase information can be obtained by interferometry or by time domain methods.<sup>5</sup> In neither of these optical frequency methods, however, can the phase of the reflected wave easily be determined, so that a true material characterization cannot be obtained—although measurements of just the refractive index do appear to be feasible.<sup>6,7</sup>

Here, we apply an alternative technique (referred to here as the Fresnel method) to characterize a planar split-ring resonator (SRR) medium, using transmission amplitude data taken at multiple angles of incidence relative to the plane of the SRRs.<sup>8</sup> In this technique, the Fresnel formulas for reflection and transmission from a continuous material interface at an angle of incidence are derived. Multiple material layers can be stacked up and the transmission through the entire stack can be found. By varying the material properties corresponding to each layer, we fit our modeled transmission spectra to the measured spectra. Fitting transmission data sets at multiple angles *simultaneously* reduces the possible ambiguity of multiple best-fit solutions, thus obviating the need for phase information.

Our metamaterial sample consists of a planar layer of gold SRRs photolithographically patterned onto a  $n$ -doped, 30  $\Omega$  cm resistivity, double-sided polished silicon wafer, spin coated with a layer of benzocyclobutene (BCB). BCB was chosen for its moderate dielectric constant, low losses in the terahertz range, and planarizing properties. It also helps with gold adhesion during the lift-off process used during the photolithography. The measured thickness of the BCB layer is 6  $\mu\text{m}$ . The resultant sample geometry is shown in the insert of Fig. 1. Transmission measurements are performed in a Bruker 66v Fourier transform infrared (FTIR) spectrometer, with the sample oriented such that  $s$ -polarized light is incident at angle  $\theta$  from the surface normal. The sample dimensions are  $1 \times 1 \text{ cm}^2$  (an array of  $277 \times 277$  split rings). Because each SRR element is inherently bianisotropic, we symmetrized the SRR array, as shown in the insert of Fig. 1—so as to eliminate magnetoelectric coupling.<sup>9</sup> The resulting metamaterial layer can then be described by an in-plane permittivity  $\epsilon_x(\omega)$  and an out-of-plane permeability  $\mu_z(\omega)$ . The transmitted light amplitude is measured as a function of frequency from 0.61 to 6.06 THz and at angles from  $\theta=0^\circ$  to  $\theta=45^\circ$ . These transmission spectra are plotted in Fig. 1, in a low resolution [ $4 \text{ cm}^{-1}$  (0.12 THz)] which excludes Fabry-Pérot (FP) fringes that arise from the Si substrate. In these spectra, there are two dominant features: an angle-dependent

<sup>a)</sup>Electronic mail: tdriscoll@physics.ucsd.edu

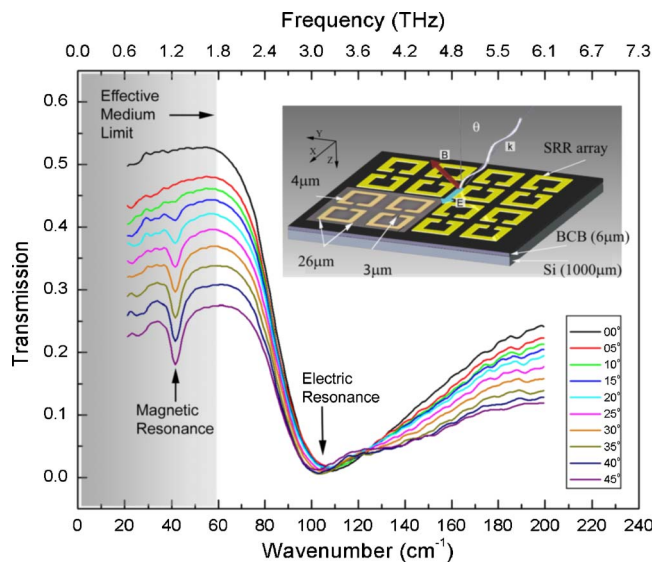


FIG. 1. (Color online) Low-resolution [ $4 \text{ cm}^{-1}$  ( $0.12 \text{ THz}$ )] transmission spectra at angles of incidence ranging from  $0^\circ$  to  $45^\circ$ . Inset: Sample geometry and polarization orientation. The lower left of four SRRs are an insert from an optical photograph, with included actual measured dimensions.

magnetic resonance at  $1.27 \text{ THz}$  and an angle-independent stronger electric resonance at  $3.03 \text{ THz}$ . The assignment of electric and magnetic to the two features comes from our polarization setup necessitating no magnetic response—but strong electric response—at  $0^\circ$ . This assignment is corroborated by previous work wherein the electric resonance always appears above the magnetic, and simulation results showing the position of the magnetic resonance (discussed below). The low-resolution spectra allow the full range of the data set (including the higher-frequency electric resonance) to be plotted with clarity. High-resolution [ $0.25 \text{ cm}^{-1}$  ( $0.008 \text{ THz}$ )] spectra—which include the FP oscillations—are plotted over a restricted range of  $0.91$ – $1.52 \text{ THz}$  in Fig. 2 (color lines) for the angles of incidence of  $\theta=0^\circ$ ,  $30^\circ$ , and  $45^\circ$ . This frequency range bounds

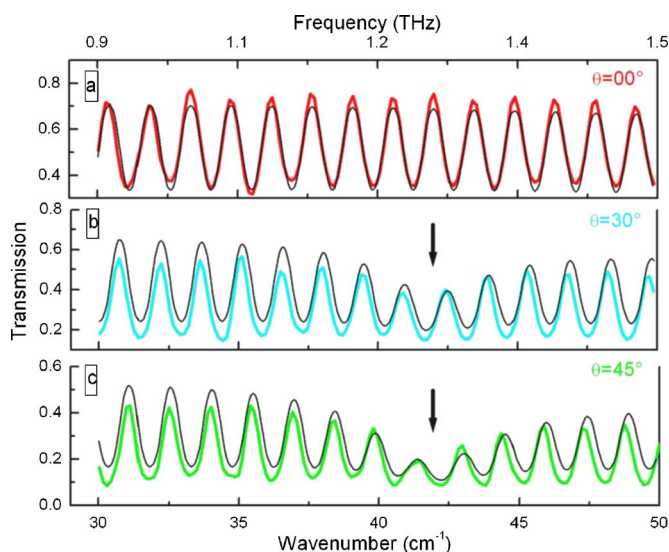


FIG. 2. (Color online) High-resolution [ $0.25 \text{ cm}^{-1}$  ( $0.008 \text{ THz}$ )] experimental transmission spectra (colored bold lines) zoomed on the magnetic resonance for  $\theta=0^\circ$  (a),  $30^\circ$  (b), and  $45^\circ$  (c). Fresnel transmission fit (thin black lines) for each angle. The position of the magnetic oscillator interaction is indicated by a black arrow.

the magnetic resonance of interest, which manifests at  $1.27 \text{ THz}$  as an angle-dependent reduction in the amplitude of the FP oscillations.

By restricting our analysis to the range over which the effective medium approximation for metamaterials can be applied<sup>1</sup> (up to  $\lambda > 5P$ , corresponding  $\sim 1.7 \text{ THz}$  in our array), we treat this sample as a simple multilayer system:  $\sim 1000 \mu\text{m}$  of silicon,  $6 \mu\text{m}$  of BCB, and a thickness of metamaterial. There is a caveat here: although the actual gold thickness of the SRR metamaterial is submicron ( $100 \text{ nm}$  gold layer), the *effective thickness* (out of plane) of the metamaterial layer has been shown to be nearly equal to the (in plane) periodicity of the SRR array.<sup>10,11,3</sup> The effective thickness is a manifestation of how far the SRR induced fields extend above and below the SRR plane ( $P=36 \mu\text{m} \rightarrow z_{\text{eff}} = \pm 18 \mu\text{m}$ ). This also means that there is an apparent overlap of the naively defined metamaterial and BCB layers. In truth, the BCB is in the immediate vicinity of the gold rings and directly modifies the local fields of the SRR. It thus becomes *part* of the optical constants of the metamaterial layer—rather than acting as its own separate layer. The effect of the BCB layer should not be “double counted,” and we perform our analysis as such.

We can find an analytical expression for the transmitted power through the multilayer sample by enforcing the continuity of the tangential components of the electric field  $E$  and magnetic intensity at the boundaries of each of the layers. The full expression for transmitted power is quite long, but the procedure for derivation can be found, and in<sup>8</sup> and in other standard texts.<sup>12,13</sup> The total transmission is a function of the layer thicknesses, the isotropic dielectric constant of the silicon, and of the in-plane electric and out-of-plane magnetic responses of the metamaterial+BCB layer.<sup>14</sup> Far-infrared values for the dielectric value of lightly doped silicon ( $\epsilon_{\text{Si}}=11.9+0.01i$ ) (Ref. 15) and BCB ( $\epsilon_{\text{BCB}}=2.5+0.01i$ ) (Ref. 16) can be readily found in literature. A control measurement on a silicon only sample using these literature values shows that our derived Fresnel transmission formula accurately models the observed transmission through natural material layers. For the frequencies treated in our analysis (those shown in Fig. 2), the higher-frequency dynamic aspects of the electric resonance can be ignored, and we reduce its full interaction  $\epsilon_x(\omega)$  to a static dielectric constant of the metamaterial layer  $\epsilon_x$ .

The spectral features arising from the metamaterial resonances are intertwined with the substrate fringes, and extracting the metamaterial  $\epsilon_x$  and  $\mu_z(\omega)$  would, in principle, require fitting to all parameters of the system simultaneously across the angle data sets, and repeating this at each frequency. Fortunately, in this work our primary interest is limited to the magnetic out-of-plane resonance, whose form for the SRR medium is known to be well approximated by the modified Lorentzian-oscillator function,<sup>17–19</sup>

$$\mu_z(\omega) = 1 - \frac{A_m \omega^2}{\omega^2 - \omega_{m0}^2 + i\omega\gamma_m}. \quad (1)$$

This allows us to make a great computational simplification: collapsing a fitting calculation at every frequency point into a single fitting for the oscillator parameters in this frequency dispersion relation. Additionally,  $\mu_x = \mu_y = 1$ , since only  $z$  components of the  $B$ -field couple to the metamaterial. To generate a fit of our model to the data, we iteratively vary the

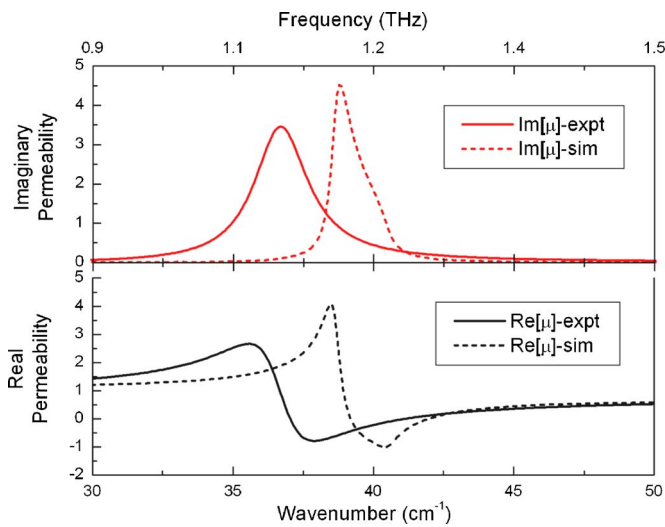


FIG. 3. (Color online) Metamaterial out-of-plane magnetic permeability for the Fresnel fit to experimental data (solid lines) and  $S$ -parameter inversion of the simulated structure (dashed).

fitting parameters for layer thicknesses, substrate and metamaterial dielectric values, and parameters in Eq. (1) to find the set of values which gives the best *simultaneous* fit to the data at  $0^\circ$ ,  $15^\circ$  (not plotted),  $30^\circ$ , and  $45^\circ$ . The real and imaginary metamaterial permeabilities generated from the fitted values of Eq. (1) are shown in Fig. 3 (solid lines). This result for permeability has a standard resonant form, becoming negative over a short range and reaching a maximally negative value of  $\mu_z = -0.8$  at 1.15 THz. The fitted values for the metamaterial and silicon layer thicknesses are  $d_{\text{MM}} = 37 \mu\text{m}$  and  $d_{\text{Si}} = 970 \mu\text{m}$ , respectively.

To check that our fit-resultant permeability curve is reasonable, we perform a finite element simulation of our metamaterial, using the commercial software MICROWAVE STUDIO. The simulation output contains enough information to directly generate the optical constants.<sup>20</sup> The possible geometry of the simulation restricts  $k$  to one of the  $x$ ,  $y$ , and  $z$  so we simulate the equivalent of  $\theta = 90^\circ$ , though this cannot in practice be performed experimentally. The permeability predicted by the simulation is overlaid in Fig. 3 (dashed lines). We find that the simulation results are in general agreement, but exhibit a sharper resonance than in our experimental sample. This is not surprising given the dampening effect of small sample defects.<sup>21</sup> The simulation-retrieved permeability peak also occurs at a higher frequency by a couple wave numbers. Some of this discrepancy may be due to the necessary assumptions made in finite element simulations, such as partial substrate inclusion. More importantly, it is known that the finite size of our unit cells will cause problems here. Our Fresnel formulation, and thus our experimentally retrieved permeability fit, relies on the validity of our assumption that the SRRs act together as a continuous material which supports collective modes rather than as individual antenna responses which occur in sparse arrays. Our sample has a periodicity of only seven times smaller than the resonant wavelength. Although this is typical for a metamaterial, previous work has indicated that the discrete medium only becomes truly indistinguishable from a continuous material at  $\sim \lambda/30$ .<sup>1</sup> Thus our model neglects any effects due to spatial dispersion in our metamaterial layer—which are cer-

tainly present given the known phase inhomogeneities<sup>3</sup> within the unit cells. The appropriate modeling approach in these conditions would be a hybrid of the Fresnel theory appropriate for continuous materials and of the antenna theory used for discrete elements, which we hope to soon develop.

To summarize, we have measured the far-infrared transmission through a split-ring-resonator metamaterial sample with an artificial (tailored) magnetic resonance. Using the Fresnel formulas and assuming an effective medium, we have formed an expression for transmission through this metamaterial at any acute angle of incidence in terms of the magnetic resonance and the other material parameters. These parameters are simultaneously fitted to experimental data at four angles, which helps to compensate for the lack of phase information. The experimentally measured permeability reaches a value of negative  $-0.8$  on resonance, and we see fairly good quantitative agreement of the permeability resonance for our SRR array with that retrieved by finite element simulation of the structure. The ability to couple quantitative experimental measurements with simulation predictions is an important tool in the ongoing research into metamaterials, and the Fresnel analysis presented here helps make this possible in frequencies ranges or situations where phase information may not be available.

<sup>1</sup>Th. Koschny, P. Markos, E. N. Economou, D. R. Smith, D. C. Vier, and C. M. Soukoulis, Phys. Rev. B **71**, 245105 (2005).

<sup>2</sup>A. F. Starr, P. M. Rye, D. R. Smith, and S. Nemat-Nasser, Phys. Rev. B **70**, 113102 (2004).

<sup>3</sup>D. R. Smith, D. C. Vier, Th. Koschny, and C. M. Soukoulis, Phys. Rev. E **71**, 036617 (2005).

<sup>4</sup>T. Driscoll, D. N. Basov, A. F. Starr, P. M. Rye, S. Nemat-Nasser, D. Schurig, and D. R. Smith, Appl. Phys. Lett. **88**, 081101 (2006).

<sup>5</sup>W. J. Padilla, A. J. Taylor, C. Highstrete, M. Lee, and R. D. Averitt, Phys. Rev. Lett. **96**, 107401 (2006).

<sup>6</sup>D. R. Smith, S. Schultz, P. Markos, and C. M. Soukoulis, Phys. Rev. B **65**, 195104 (2002).

<sup>7</sup>V. M. Shalaev, W. Cai, U. K. Chettiar, H.-K. Yuan, A. K. Sarychev, V. P. Drachev, and A. V. Kildishev, Opt. Lett. **30**, 3356 (2005).

<sup>8</sup>T. Driscoll, D. N. Basov, W. J. Padilla, J. J. Mock, and D. R. Smith, Phys. Rev. B (in press).

<sup>9</sup>D. R. Smith, D. A. Schurig, and J. J. Mock, Phys. Rev. E **74**, 036604 (2006).

<sup>10</sup>B. Popa and S. A. Cummer, Phys. Rev. B **72**, 165102 (2005).

<sup>11</sup>M. Gorkunov, M. Lapine, E. Shamonina, and K. H. Ringhofer, Eur. Phys. J. B **28**, 263 (2002).

<sup>12</sup>Max Born and Emil Wolf, *Principles of Optics* (Pergamon, London, 1970), Ch 1.6.

<sup>13</sup>R. M. A. Azzam and N. M. Bashara, *Ellipsometry and Polarized Light* (Elsevier, Amsterdam, 1977), Ch. 4.7.

<sup>14</sup>T. Koschny, M. Kafesaki, E. N. Economou, and C. M. Soukoulis, Phys. Rev. Lett. **93**, 107402 (2004).

<sup>15</sup>E. V. Loewenstein, Donald R. Smith, and R. L. Morgan, Appl. Opt. **12**, 2 (1973).

<sup>16</sup>Dow Chemicals Product datasheet: <http://www.dow.com/cyclotene/solution/highfreq.htm>

<sup>17</sup>J. B. Pendry, A. J. Holden, W. J. Stewart, and I. Youngs, Phys. Rev. Lett. **76**, 4773 (1996).

<sup>18</sup>J. B. Pendry, A. J. Holden, D. J. Robbins, and W. J. Stewart, IEEE Trans. Microwave Theory Tech. **47**, 2075 (1999).

<sup>19</sup>D. R. Smith, J. J. Mock, A. F. Starr, and D. Schurig, Phys. Rev. E **71**, 036609 (2005).

<sup>20</sup>G. Dolling, C. Enkrich, M. Wegener, C. M. Soukoulis, and S. Linden, Science **312**, 892 (2006).

<sup>21</sup>M. V. Gorkunov, S. A. Gredeskul, I. V. Shadrivov, and Y. S. Kivshar, Phys. Rev. E **73**, 056605 (2006).